IEEE Access
Multidisciplinary | Rapid Review | Open Access Journal

Received April 27, 2018, accepted May 26, 2018, date of publication June 12, 2018, date of current version July 6, 2018.

Digital Object Identifier 10.1109/ACCESS.2018.2846589

Proposal for Optimization of Spool Valve Flow Force Based on the MATLAB-AMESim-FLUENT Joint Simulation Method

CHEN QIANPENG, JI HONG, ZHU YI, AND YANG XUBO
College of Energy and Power Engineering, Lanzhou University of Technology, Lanzhou 730050, China

Corresponding author: Ji Hong (jihong@lut.cn)

This work was supported by the National Natural Science Foundation of China under Grant 51575254 and in part by the Special Fund Project of Strategic and New Industry Development of Jiangsu Province in 2016—The Research and Industrialization of Core Technology of Hydraulic Pump and Valve Applied in High-End Construction Machinery.

ABSTRACT This paper focuses on the open-center multi-way valve used in loader buckets. To solve the problem of excessive flow force that leads to spool clamping in the reset process, joint simulations adopting MATLAB, AMESim, and FLUENT were carried out. Boundary conditions play a decisive role in the results of computational fluid dynamics (CFD) simulation. However, the boundary conditions of valve ports depend on the hydraulic system's working condition and are significantly impacted by the port area, which has always been neglected. This paper starts with the port area calculation method, then the port area curves are input into the simulation hydraulic system, obtaining the flow curves of valve port as output, which are then applied as the boundary conditions of the spool valve CFD simulation. Therefore, the steady-state flow force of the spool valve is accurately calculated, and the result verifies the hypothesis that excess flow force causes spool clamping. Based on this, four kinds of structures were introduced in an attempt to improve the situation, and simulating calculation and theoretical analysis were adopted to verify the effects of improvement. Results show that the four structures could reduce the peak value of flow force by 17.8%, 60.6%, 61.6%, and 55.7%, respectively. Of the four, structures II, III, and IV can reduce the peak value of flow force to below reset spring force value, thus successfully avoiding the spool clamping caused by flow force.

INDEX TERMS Spool clamping, port area calculation, joint simulation, CFD, steady-state flow force, improved structure.

I. INTRODUCTION

When designing hydraulic valves, performance parameters such as flow, pressure, etc. are usually taken to determine its structure, while the effect of flow force on the working process is neglected, resulting in unsatisfactory force conditions of some spool valves during actual practice, affecting its operating performance and control characteristics [1]. Excessive flow force makes managing the main-control spool valve's operating characteristics a difficult task, resulting in problems such as handle clamping, decrease of operating sensitivity, the actuator's motion characteristics not yielding expected results, etc. Accurate and precise calculations of the spool valve's flow force and solutions for reducing it provide both sound evidence for a reasonable hydraulic spool valve design and improvement in the sensitivity and life of control components. It is of vital importance and significant practical value for the operability and safety of construction machinery.

Over a course of many years, experts around the world have conducted studies on hydraulic valve power and its control features [2]–[9]. Zhang *et al.* [10] presented a study with solid evidence on three different flow field structures, providing both reasonable designs of hydraulic spool valves and ways to improve the sensitivity and life of control components. It is an important and remarkable development for spool valves of electro-hydraulic proportional valve by means of CFD. Qing *et al.* [11] applied User-Defined Function in Fluent to link the fitting function with flow field calculation, and used sliding mesh to calculate the variation characteristics of flow force in the opening process. Herakovič [12] investigated the flow force of combined electro-hydraulic proportional valves, analyzed singular flow force acting on various stress wall surfaces of the spool valve, and improved spool valve structure. Employing contrast experiments, he proved that the improved structure effectively reduced the

peak value of flow force. Borghi *et al.* [13], also by means of CFD, performed numerical simulations and experiments of three kinds of common spool valve bodies with flow force compensation, verifying that the improved structure could indeed reduce flow force. Lisowski *et al.* [14] focused on the 3-section, 4-way proportional directional control valve, researched the characteristics of flow force through test and analysis, and connected the A and T ports, causing the flow force of spool valves to reduce significantly. For purposes of experimental validation, a test bench was built. The test results confirmed the data collected from simulations, finding flow capacity enhanced by 45% thanks to the improved structure. Lisowski *et al.* [15] also conducted research concerning the pressure-flow property of multi-section proportional directional control valves using CFD, and then built a test bed for the flow field. The results show that flow force is compensated when the flow field is changed or a groove is added. In addition, spring stiffness upon reset also affects the flow rate's allocation property. When a high level of control precision is not required, pressure compensation methods can avoid the addition of unnecessary components; these are simple and feasible methods which can be implemented when attempting to control flow force.

Existing works concerning flow field simulation generally simplified inlet flow and pressure as a fixed value, thus affecting the accuracy of simulation results. In this research, the calculation program for port area is written and the hydraulic system of the loader bucket is established by means of joint simulation applying MATLAB, AMESim and FLUENT, obtaining the flow curve of port P-T in the spool valve's reset process. Using the flow curve as the inlet boundary condition for simulation, the steady-state flow force curve of the spool valve is obtained. It is proved that spool clamping does exist in the reset process of spool valves, which is mainly caused by excess flow force. To solve the problem of spool clamping, four kinds of structures are proposed, which effectively reduce the peak value of flow force, as well as avoid spool clamping.

II. SIMULATION OF RESET PROCESS CONCERNING BUCKET CONTROL HYDRAULIC SYSTEMS

A. RESET PROCESS OF BUCKET CONTROL VALVE

The loader's 6-port 3-way open center multi-way valve is different in that the bucket spool and the boom spool cannot operate simultaneously. When one spool is being used, the other is in center unloading position. When both are in neutral position, the passage linking ports P and T is clear. The multi-way valve's three dimensional structure is as shown in Figure 1.

The bucket spool experiences spool clamping during reset, and as only observation of its reset process is needed, the multi-way valve's structure diagram is simplified. When the bucket is functioning, the boom is in neutral position, therefore the boom is simplified as port T. Moreover, for convenience of study, the two ports (both port Ts) positioned

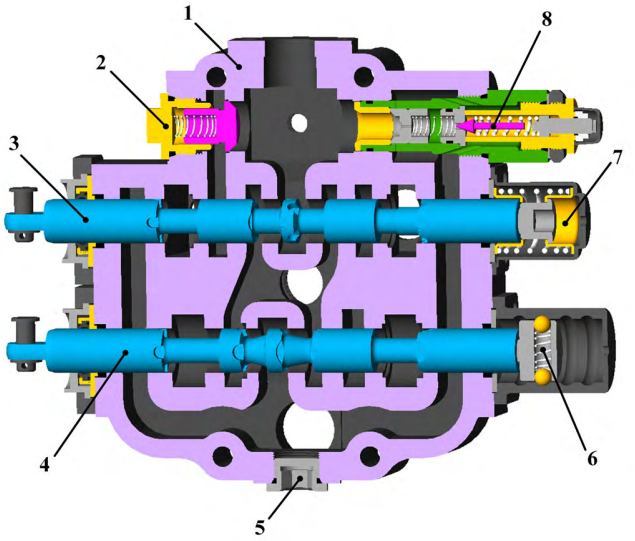

1—valve body; 2—check valve; 3—bucket spool valve; 4—boom spool valve; 5—screw plug; 6—boom reset spring mechanism; 7—bucket reset spring mechanism; 8—safety valve

FIGURE 1. Three dimensional structure diagram of loader's open center multi-way valve.

in the middle of the spool are separately marked as ports T_1 and T_2. Figure 2(a) shows a simplified schematic diagram of the bucket control valve, with the "*s*" representing the position of the spool. In addition, P-T, as mentioned in this paper, can be used to refer to P-T_1 or P-T_2, as well as P-T_1 and P-T_2. This is visible in Figure 2(a).

Figure 2(b) is a diagram of the bucket control valve's hydraulic system. A comparison of Figures 2(a) and 2(b) show that when the spool valve opens(*s* moves from 0mm to −13mm) and reaches a valve overlap of 3.5mm, ports P-A and B-T are linked respectively, the capacity of the oil cylinder's rodless chamber grows, the bucket's oil cylinder is lifted, and the bucket flips upward. When the bucket flips to extreme position, the capacity of the rodless chamber no longer changes, the oil pressure of line P-A increases and is slightly higher than that of the relief valve, thus opening it, and oil from port P returns to port T via the relief valve. If the control lever is released, the spool valve automatically returns from extreme position to neutral position(*s* moves from −13mm to 0mm) under reset spring force, ports P-A and B-T shut, the bucket's oil cylinder does not shift, and oil from port P flows through the middle of the spool valve to port T. In the spool valve's reset process, oil always flows from port P to port T, but the way in which the two ports are connected varies, i.e. in gradual transition from the relief valve to the port situated at the middle of the spool valve.

B. AREA COMPUTATION OF P-T_1 AND P-T_2 PORTS BASED ON MATLAB

Further study on spool valve reset process reveals the spool valve's return travel to be 13mm. During this process, port P-T_1 gradually opens, and after an interval of overlap, upon

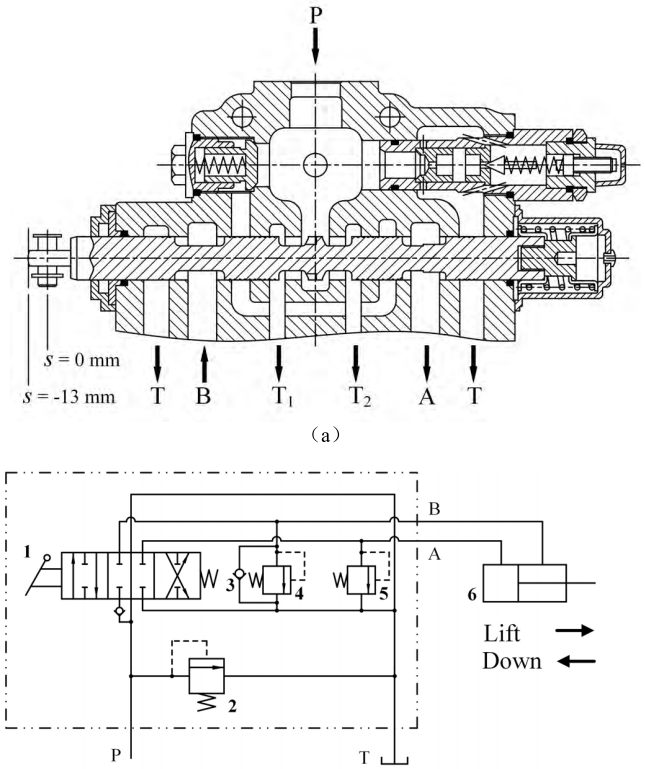

FIGURE 2. Structure diagram and hydraulic system of loader's control valve. (a) Simplified schematic diagram of bucket control valve. (b) schematic diagram of bucket control valve's hydraulic system.

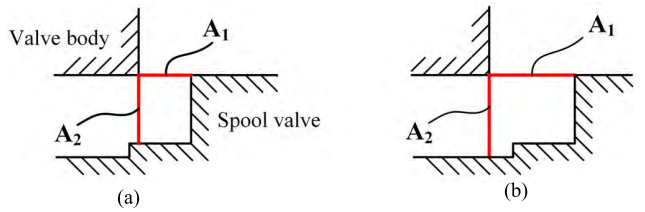

FIGURE 3. Axial section of two-step throttle. (a) Opening groove. (b) Fully opened groove.

reaching maximum opening size, port P-T_2 gradually shuts. In the open and shutting processes, as the groove is critical to the valves' control characteristics, a calculation of valve port area is needed.

In recent years, research on calculation methods concerning port area has made great progress [16], [17], Ji's research team in particular [18], [19]. Based on existing research, and taking into consideration the stage after the U groove is fully opened, a brief simulation of the calculation methods for port area were deduced. The U groove has typical two-step throttle properties (as shown in Fig.2), the valve port flow area A_U is calculated by A_1 in series with A_2 [20], calculation is divided into two cases: opening groove and fully opened groove. The computational principle employed is Formula (1), as shown below.

$$A_U = \frac{1}{\sqrt{\frac{1}{A_1^2} + \frac{1}{A_2^2}}} = f(A_1, A_2) \tag{1}$$

Analysis on valve port area variation characteristics. The central section of Figure 4 depicts schematic diagrams of matching between the valve core and body. *I*, *J*, and *K* are partial sectioned views of the valve ports.

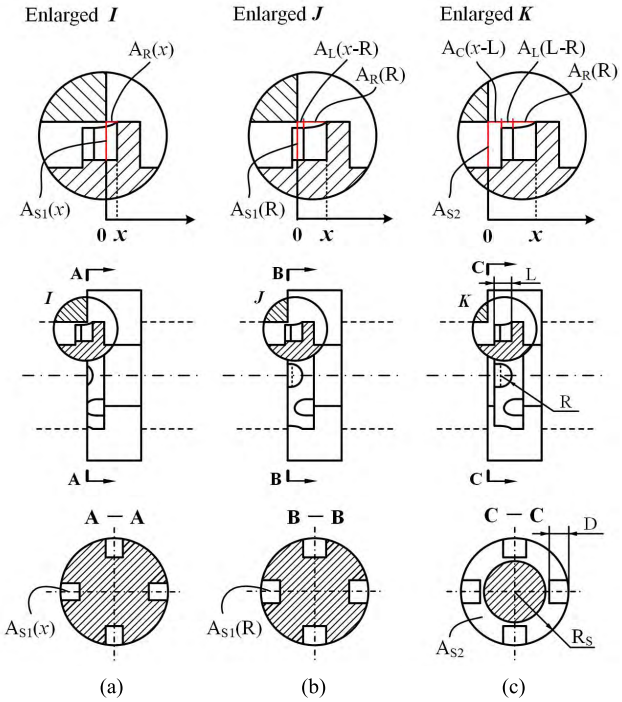

FIGURE 4. Different characteristics of valve port with U groove in three stages. (a) 0mm≤ *x* <3mm. (b) 3mm≤ *x* <4.5mm. (c) *x* ≥4.5mm.

Above *I*, *J* and *K* are enlarged diagrams of the valve ports, with units constituting valve port area of each stage marked. Also marked is a one-dimensional axial coordinate of variable "*x*," with the valve body's matching surface serving as origin, and the valve port area's length of projection on the valve core axial direction serving as variable "*x*" in its computing function. Below *I*, *J* and *K* are shift out sections cut along the matching surface of the valve body. Also marked in Figure 4 are characteristic parameters of the U groove.

The opening process of port P-T_1 (*x* moves from 0mm to 9.5 mm) can be divided into three stages according to different characteristics which appear in the variations of valve port area. Each stage requires a different computing method for area. As shown in Figure 4, in the fully opened stage of the opening process of the port, when valve port area is determined as a constant, and the different values of area in the current stage are represented by a term including unknown variable "*x*", the following computing methods for valve port area in each stage are obtained:

(1) As shown in Figure 4(a), when the valve port's opening size is 0mm $\leq x <$ 3mm, the U-shaped groove's

semi-circular port opens progressively. At this point, A_1 is the total area of the four gradually changing arc forms', and A_2 is the total area of the four gradually changing rectangles'. A_1 and A_2 can be indicated as:

$$A_1 = 4A_R(x) \tag{2}$$

$$A_2 = 4A_{S1}(x) \tag{3}$$

(2) As shown in Figure 4(b), when the valve port's opening size is 3mm$\leq x <$ 4.5mm, the U-shaped groove's semi-circular port is fully open, and the hind of the rectangular port progressively opens. At this point, A_1 is the total area of the four gradually changing U-shaped grooves', and A_2 is the total area of the four unchanging rectangles'. A_1 and A_2 can be indicated as:

$$A_1 = 4A_R(R) + 4A_L(x - R) \tag{4}$$

$$A_2 = 4A_{S1}(R) \tag{5}$$

(3) As shown in Figure 4(b), when the valve port's opening size is 4.5mm $\leq x \leq$ 9.5mm, the U-shaped groove is fully open, the valve port completely open. At this point, A_1 is the sum of the combined area of the four whole U-shaped grooves plus the surface area of a cylindrical form, and A_2 is the area of a ring-shaped form. A_1 and A_2 can be indicated as:

$$A_1 = 4A_R(R) + 4A_L(L - R) + A_C(x - L) \tag{6}$$

$$A_2 = 4A_{S2} \tag{7}$$

The closing process of port P-T_2 and the opening process of port P-T_1 in the third stage (with $x \geq$ 4.5mm) are symmetric. Suppose the opening degree of valve port P-T_2 is "y"; when 13.5mm $\geq y \geq$ 9.5mm, the computing method for valve port area is similar to that in (6) and (7). A_1 and A_2 can be indicated as:

$$A_1 = 4A_R(R) + 4A_L(L - R) + A_C(y - L) \tag{8}$$

$$A_2 = 4A_{S2} \tag{9}$$

Where:

L is the depth of the U groove;

R is the radius of the characteristic circle of the U groove;

$A_R(x)$ is the radial port area function of the semicircle part of the U groove;

$A_L(x)$ is the radial port area function of the rectangle part of the U groove;

$A_C(x)$ is the radial port area function when the U groove is fully-open;

$A_{S1}(x)$ is the axial port area function of the U groove;

$A_{S2}(x)$ is the axial port area function when the U groove is fully-open.

As for the actual spool valve used in this study, the U groove parameters are as follows: D=4.14mm; R=3mm; L=4.5mm; R_S = 14mm.

For the final step, A_1 and A_2 of P-T_1 and P-T_2 are used in series calculation according to formula (1), and the equivalent area curves of P-T_1 and P-T_2 in the spool valve's reset process can be obtained.

With reference to the calculation formula for port area in the reset process of the valve core, the calculation program for port area was written using MATLAB, and visual interface was customized to obtain the area curves of ports P-T_1 and P-T_2 (as shown in Fig. 5).

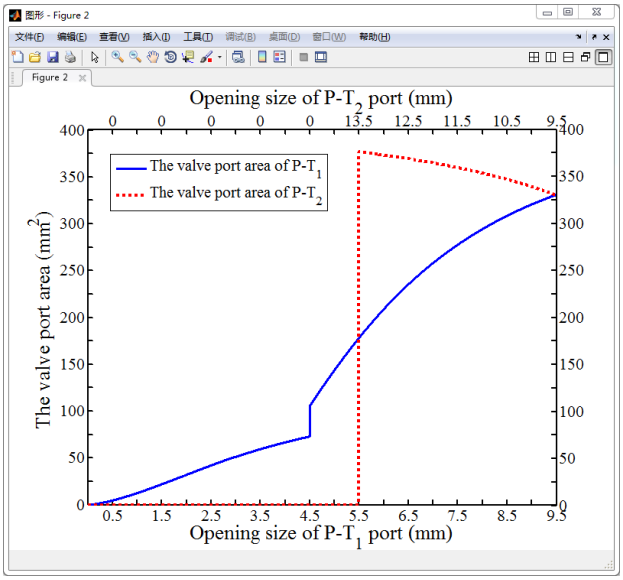

FIGURE 5. Area curves of P-T_1 and P-T_2 ports.

From Figure 5, we can see that in the valve core's reset process, when P-T_1's opening size is 0mm<x≤5.5mm, port P-T_2 is shut. When port P-T_1's opening size is 5.5mm<x≤9.5 mm, port P-T_2's opening size gradually reduces from the maximum 13.5mm until the valve core hits neutral position, at which point port P-T_1 and P-T_2's opening size are both 9.5mm. In addition, when port P-T_1's opening size goes slightly over 4.5mm, there is an obvious leap in its area; a comparison of Figures 4(b) and 4(c) show that this is when the valve port is in critical position, with the U-shaped groove fully open and the port just entirely opened, causing A_1 and A_2's areas to increase suddenly; a series calculation of A_1 and A_2 causes an increase in equivalent valve port surface also. The area curves shown in Figure 5 will be used as given parameters in the AMESim hydraulic simulation system as the next step.

C. SIMULATION OF HYDRAULIC SYSTEM BASED ON AMESim

With reference to the multi-way valve bucket's structure and hydraulic system shown in Fig.2, we established the model of its hydraulic system using AMESim (as shown in Fig.6), then simulated the reset process of the spool valve. Because of the U-shape throttling groove of ports P-T_1 and P-T_2, the area curve of port P-T is nonlinear in the reset process, thus the 'hydraulic spool with specific orifice' module is needed. Then the area curves using MATLAB are input to the module to ensure accurate flow curves. Other main parameters of the system are shown in table I.

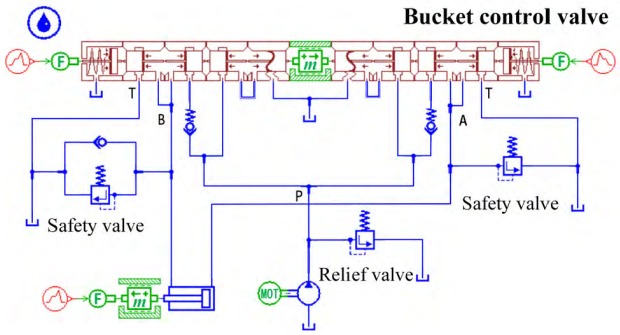

FIGURE 6. AMESim model of bucket control valve.

TABLE 1. Key parameters OF AMESim model.

Component	Parameter/(Unit)	Value
Hydraulic pump	Displacement /（mL/r）	150
Motor	Rotate speed /（r/min）	2200
Reset spring	Spring stiffness /（N/mm）	2.64
Safety valve	Setting pressure /（MPa）	25
Relief valve	Setting pressure /（MPa）	18
Cylinder piston	Large-diameter /（mm）	180
	Small-diameter /（mm）	100
	Load pressure/（MPa）	4

Through simulations applying AMESim software, with conditions being load pressure of under 4MPa, correlations between control of spool valve position and the following were obtained: oil cylinder actuation, spool valve port flow, and relief valve overflow.

It can be derived from Figure 7 that during the interval of 0s to 1.8s, the spool valve moves from 0mm to −13mm, port P-T gradually shuts after a period of constant flow, ports P-A and B-T open progressively, some oil from port P is directed to the oil cylinder's rodless chamber via port A, oil from the cylinder's rod chamber returns to port T via port B, causing the bucket oil cylinder's piston to extend from initial position after 1s; as port P-T shuts, ports P-A and B-T reach maximum flow.

During the interval of 3.9s to 5s, the spool valve maintains maximum opening position at −13mm, causing bucket oil cylinder piston to reach maximum travel position; oil no longer flows through the two cylinder chambers, ports P-A and B-T have a flow rate of 0L/min, and oil from port P overflows via the relief valve.

During the interval of 5s to 8s, the spool valve returns from −13mm to 0mm, the oil cylinder piston still maintains maximum stroke position, thus causing port P-A and B-T's flow rate to be 0L/min. What differs from the previous interval is that this time the valve port in the middle of the spool valve opens progressively, part of the oil at the pump port flows through the center of the spool valve to port T, with the rest overflowing through the relief valve. When port P-T opens to a certain degree, the relief valve shuts, and port P-T reaches maximum flow. In this process, port P-T's

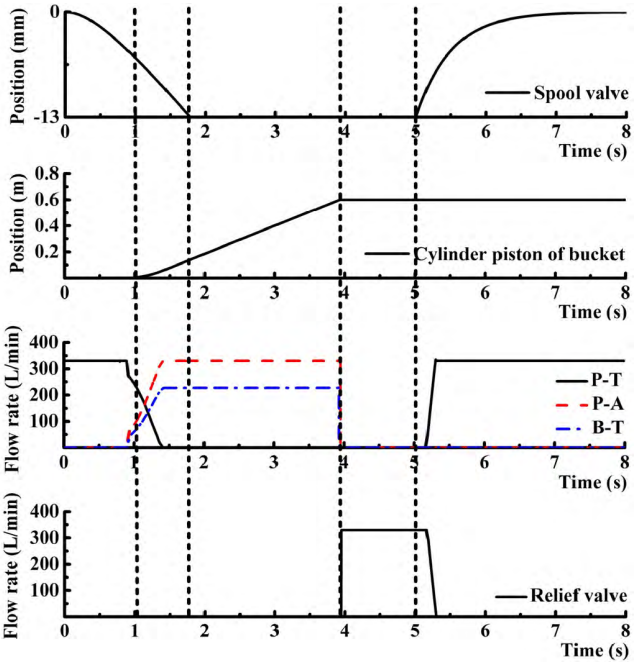

FIGURE 7. Relations between spool valve position, oil cylinder position, flow of spool valve and flow of relief valve.

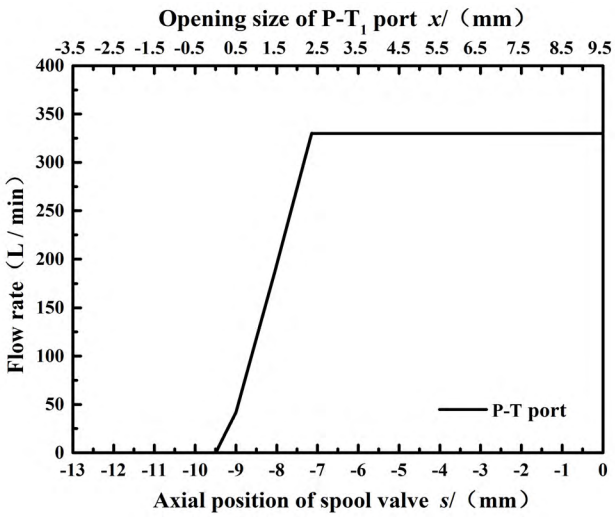

FIGURE 8. Port P-T's flow curve in the spool valve's reset process.

flow curve characteristics are determined by the relief valve's pressure setting, with load being irrelevant. Therefore when using AMESim to construct hydraulic systems, leaving out the bucket's mechanical structure and only loading a constant load of 4MPa is of no effect on port P-T's flow in the spool valve's reset process.

According to analysis, in the reset process, the flow force of the spool valve comes only from port P-T, which is generated by ports P-T_1 and P-T_2.

In the spool valve's reset process, when corresponding the valve core's position and port P-T's opening size, the relation between port P-T's flow rate and the port's opening size are

as shown in Figure 8. It should be noted that the flow curve shown here is not a constant value, which is something easily neglected in flow field simulations incorporating various opening size of the port. The flow curve here will serve as the inlet boundary condition in the next step: computing the spool valve's flow force in accordance with the valve port's different opening sizes.

III. FLOW FIELD MODELING AND FLOW FORCE CALCULATION OF SPOOL VALVE

A. CFD MODELS AND MESHING

To study the impact of flow force on spool clamping, the flow field between port P and port T is regarded as control volume; 3D flow field models with 10 valve port opening sizes ranging from 0.5mm to 9.5mm are built, and flow field simulation as well as flow force calculation are carried out.

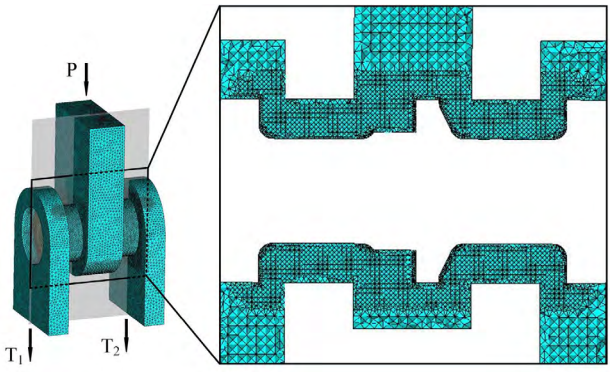

FIGURE 9. Meshed fluid zone geometry of P-T port of the spool valve.

ICEM CFD CODE is employed to generate unstructured mesh [21]. To ensure precision of calculation, ''Mesh Density'' is used to refine mesh in the narrow zone of the flow field domain. Fig.9 shows meshed fluid zone geometry of port P-T of the spool valve, and grid layers are guaranteed to be above 5. The model is built with a mesh of 1860509 cells, with worst mesh quality being 0.3, fulfilling requirements for calculation.

B. CALCULATION CONDITIONS

As of now, in hydraulic element design and research, CFD (Computational Fluid Dynamics) is the most often used tool [22]–[26]. The accuracy of simulation methods is constantly being enhanced, which provides favorable conditions for the research of flow force. FLUENT CODE was used to perform the simulation, and the standard turbulence k-ε model was also adopted. The fluid used was 46# hydraulic oil, which is incompressible Newton fluid. Oil density is 860kg/m^3, and oil viscosity is 4×10^{-5}m^2/s. The hydraulic diameter of inlet port P was set at 25.54 mm, and the outlet ports T_1 and T_2 both 16.4 mm. The flow curves of P-T ports (as shown in Fig.8) were discretized as the inlet boundary conditions under different opening sizes; outlet pressures were all set at 0.5 MPa.

C. RESULTS AND DISCUSSION

The flow force curve runs above the x-axis and in opposite directions with the spool valve's reset direction. For convenience of comparison, reset spring force (moving in the same direction as the spool valve's reset direction) will also be drawn above the x-axis. Besides, when the reset spring is in its limiting position, the pre-compression force is 149.5±5N; when it is in neutral position, the pre-compression force is 112.5±5N, and according to Hook's Law, reset spring force in reset position is obtained (as shown in Fig.10). In addition, Fig.10 also shows that when the valve's opening size is 2.5mm, reset spring force is 132.4N, while the flow force of P-T is 197.4N, which is greater than reset spring force. It can be inferred that excess flow force is the main reason for causing spool clamping in the reset process.

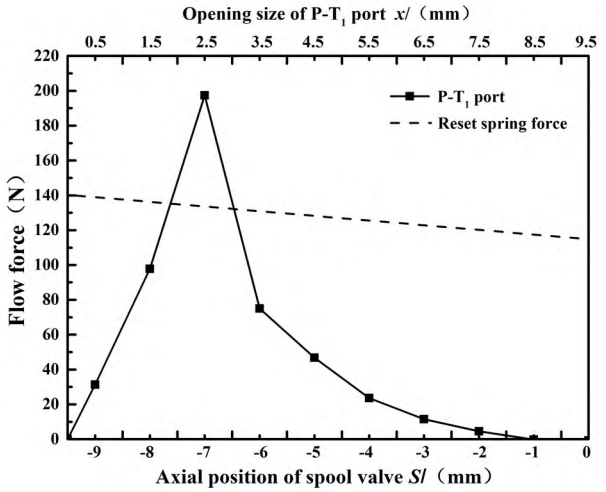

FIGURE 10. Flow force curve of the original structure.

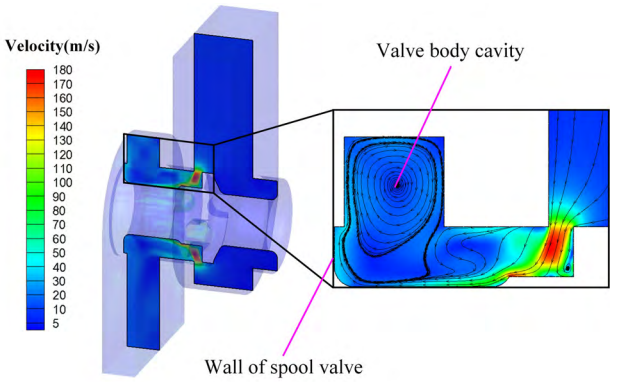

FIGURE 11. Velocity magnitude contours of original structure with opening size of P-T_1 port at 2.5mm.

To uncover the reason for excess flow force in the reset process, the flow field model is analyzed when flow force reaches peak value under the condition of port P-T_1's opening size being 2.5mm. The local velocity section is shown in Fig.11, with flow in the high pressure cavity being stable and velocity

being low. When the valve opening is rather small, high-speed jet stream is inevitably produced, which results in kinetic energy being greater in the low pressure cavity.

We can see from the direction and distribution of the streamline that when jet stream enters the low pressure cavity, it makes direct impact on the spool valve wall along the valve rod wall surface. Consequently, velocity and direction of jet stream changes and flows into the ring cavity of the valve body. Then, flow force is applied to the spool valve, which is shown through the change of spool valve motion state, which is why flow force can cause spool clamping.

IV. STRUCTURE IMPROVEMENTS

An abundance of simulations and research show that changing the inner structure of the valve can have a significant impact on the characteristics of pressure, flow and force [27]–[32]. Thus so, improvement of structure is the most direct and effective way to reduce flow force. The key to improving the characteristics of the spool valve is to reduce the peak value of flow force [33], which may be reduced if the impact on the spool valve wall is dampened by improving the structure of the valve. It is for this reason that we introduce four improved structures, and obtain by simulation streamline distributions and velocity magnitudes.

A. IMPROVED STRUCTURE I: CONE STEM SPOOL

To solve the problem of excess flow force in the original structure, improved structure I is introduced. The columned valve stem is reshaped to the conical valve stem (as shown in Fig.12). Such structure is adopted with the aim of channeling jet stream into the valve body through the conical surface, which reduces impact on the spool valve wall, thus obtaining the effect of decreased flow force.

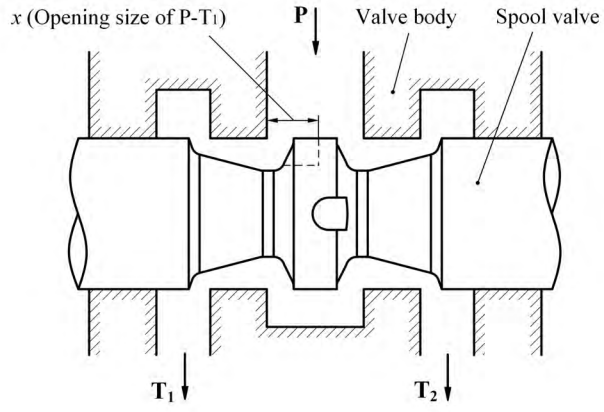

FIGURE 12. Improved structure I diagram.

According to computed results, in comparison with the original structure, the peak value of the improved structure I's flow force decreased, but force value is still greater than that of reset spring force (as shown in Fig.20), which may lead to spool clamping in the reset process.

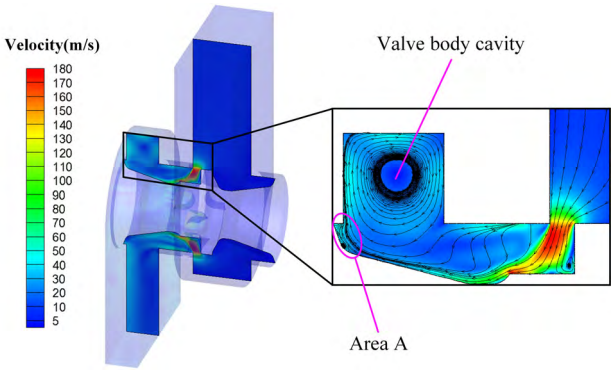

FIGURE 13. Velocity magnitude contours of improved structure I with opening size of port P-T_1 at 2.5mm.

Fig.13 shows velocity magnitude contours of the improved structure I when the opening size of port P-T_1 is 2.5mm. Streamline distributions and velocity magnitudes show that jet stream is channeled into the valve body, but some uneven streamlines and vortexes are formed in 'Area A', which causes not only energy loss, but also makes it difficult for jet stream to be smoothly channeled into the valve body. As a result, the achieved effect of decreasing improved structure I's flow force is destroyed, which is why, though widely used, structure I still cannot avoid the problem of spool clamping in application.

Thus we may assume that if the flow field of area A is retrofitted, the jet stream can smoothly channel into the valve body, and then the peak value of the spool valve's flow force may be decreased effectively.

B. IMPROVED STRUCTURE II: RING CAVITY INSIDE THE VALVE BODY

To solve the problem of non-ideal effects with improved structure I, a further improved structure II is introduced, still using improved structure I's conical valve stem for the valve core, and a couple of angular grooves are slotted in the valve body cavity, (as shown in Fig.14) to improve flow control of the conical valve stem.

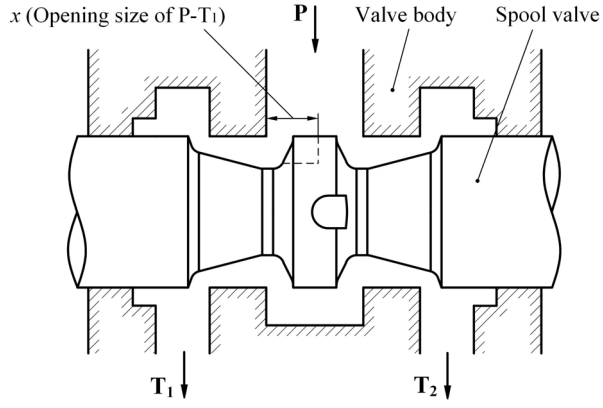

FIGURE 14. Improved structure II diagram.

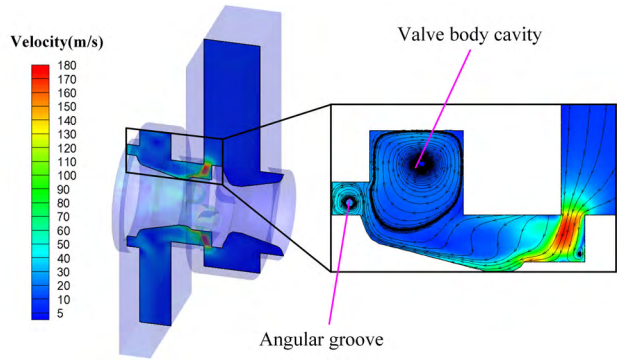

FIGURE 15. Velocity magnitude contours of structure II with opening size of port P-T_1 at 2.5mm.

Computed results show that the improved structure II can reduce flow force to below the value of reset spring force (as shown in the Fig.20). The effect is obvious.

Fig.15 shows velocity magnitude contours of the improved structure II when the opening size of port P-T_1 is 2.5mm. The streamline distributions and velocity magnitudes show that the jet stream is divided in two; one is channeled to the angular groove and forms a vortex, the other is channeled into the valve body cavity and forms a larger vortex. The improved structure II can smoothly channel jet stream into the valve body and also avoid impact with the spool valve wall, thus achieving the expected effect of decreasing the peak value of flow force.

C. IMPROVED STRUCTURE III: FLUID JET GUIDANCE BAFFLE

To solve the problem of excess flow force in the original structure, improved structure III is introduced. A kind of ring-baffle is reinforced on the valve stem, and then simulation optimization is employed to obtain the axial position and feature size of the ring-baffle [34] (as shown in Fig.16).

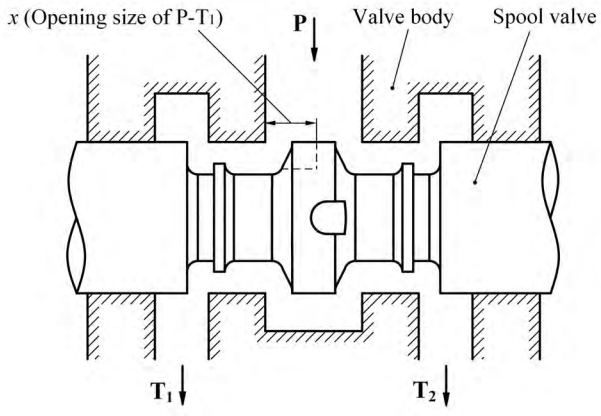

FIGURE 16. Improved structure III diagram.

According to computed results, improved structure III can reduce flow force to below the value of reset spring force (as shown in Fig.21) to obvious effect.

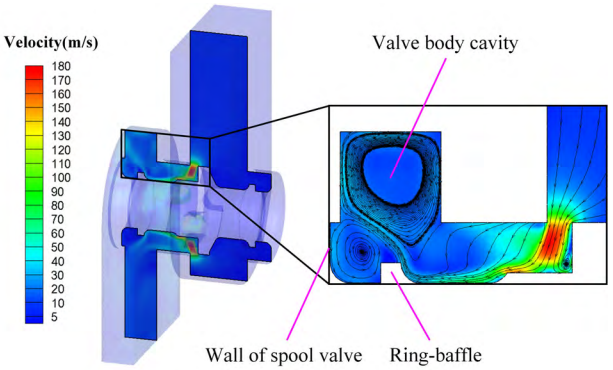

FIGURE 17. Velocity magnitude contours of structure III with opening size of port P-T_1 at 2.5mm.

Fig.17 shows velocity magnitude contours of improved structure III when the opening size of port P-T_1 is 2.5mm. The streamline distributions and velocity magnitudes show that jet stream is channeled into the valve body cavity by the ring-baffle, simultaneously forming a vortex at the hind of the ring-baffle, thus dampening impact on the spool valve wall, achieving the expected result of decreasing the peak value of flow force.

D. IMPROVED STRUCTURE IV: RING-STEP STEM

Improved structure III can effectively decrease the peak value of flow force, but when the processing technology is taken into consideration, the ring-baffle structure loses its advantage. It is for this reason that the improved structure IV is introduced, in which a kind of ring-step structure is used to replace the ring-baffle structure (as shown in Fig.18).

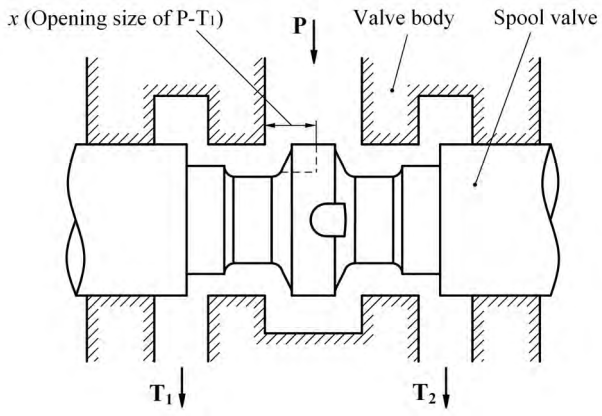

FIGURE 18. Improved structure IV diagram.

According to computed results, the improved structure IV can reduce flow force to below the value of reset spring force (as shown in Fig.21), the effect being obvious.

Fig.19 shows velocity magnitude contours of the improved structure IV when the opening size of port P-T_1 is 2.5mm. The streamline distributions and velocity magnitudes show that jet stream is channeled into the valve body cavity by the

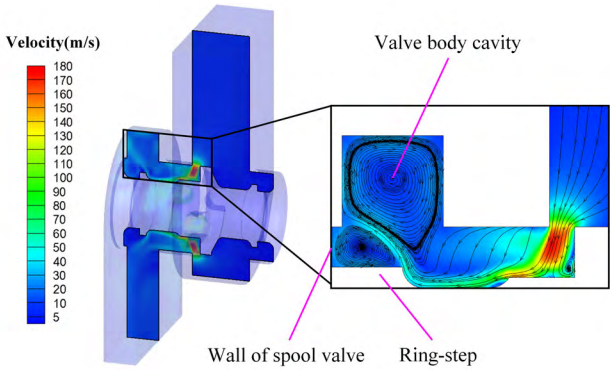

FIGURE 19. Velocity magnitude contours of structure IV with opening size of port P-T_1 at 2.5mm.

ring- step, then impact on the spool valve wall is reduced, achieving the expected result of a decreased flow force peak value.

V. COMPARISON AND ANALYSIS OF FLOW FORCE OF IMPROVED STRUCTURE

Results of flow force of the original structure are compared with reset spring force and flow force of structures I and II. As shown in Fig.20, the reference line is set at vertical coordinate 0N. Flow force and spring force are represented similarly to that in Figure 10. Flow force below the reference line termed overcompensate flow force, the overcompensate flow force and the spool valve's reset have the same direction, which needs to be observed.

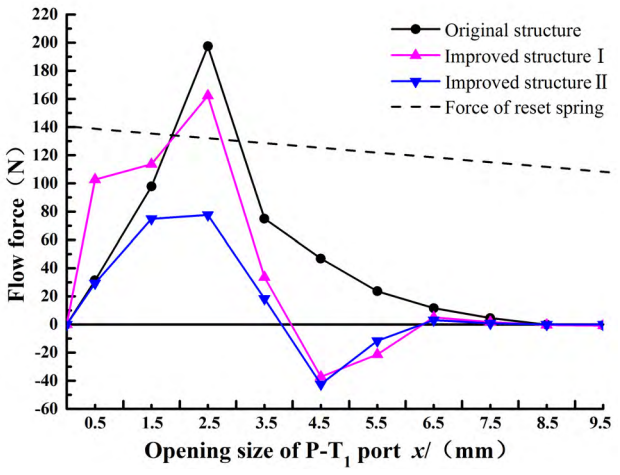

FIGURE 20. Curves of flow force of original structure, Structure I and structure II.

Fig.20 shows that the peak value of the improved structure I and II's flow force are 162.3N and 77.7N respectively. The peak value of improved structure I's flow force is still greater than reset spring force, which is non-ideal, but structure II obtained ideal improvement.

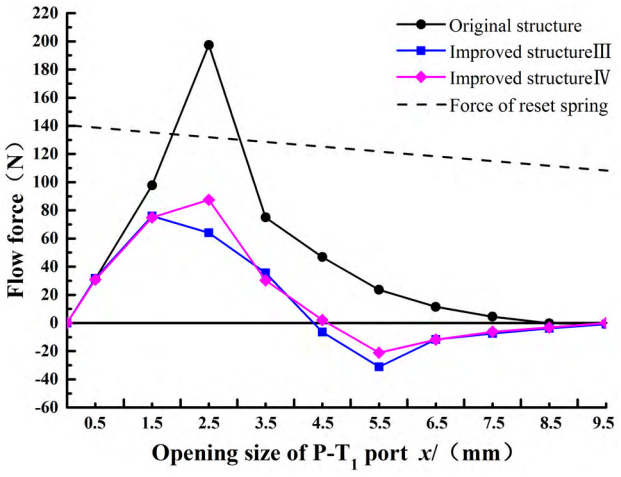

FIGURE 21. Curves of flow force of original structure, Structure III and structure IV.

The flow force of the original structure is compared with the reset spring force and flow force of structures III and IV. The results are shown in Fig.21.

Fig.21 shows that the peak value of improved structure III's flow force is 75.9N and that improved structure IV's is 87.5N. The peak values of the flow forces of improved structures III and IV are both lower than reset spring force, which brought about significant improvement.

As shown in Fig.8, Fig.20, and Fig.21, the valve port's flow rate reached maximum value when corresponding with the opening size of 2.5mm, while the flow forces of improved structures I, II, and IV all reached peak values. Also, the peak value of improved structure III appears when the opening size is 1.5mm, which can be calculated as roughly 2.5mm. We may come to the conclusion that in the reset process, when the shape of the valve port is not changed, the peak value of flow force is always reached under the specific conditions of large flow and small opening, no matter how the structures of the valve core and body are changed.

Furthermore, as shown in Fig.20 and Fig.21, when the opening size is 4.5mm, improved structures I, II, III, and IV all produce overcompensate flow force, moving in the same direction as the spool valve's reset direction. This is because improvement of the valve rod increased the spool valve's flow-through resistance, causing pressure within the chamber to rise and the spool valve's pressure surface to endure more pressure. Overcompensate flow force within a certain range will expedite the spool valve's reset process, which is efficient for preventing spool clamping; but overcompensate flow force will cause the spool valve to reset too fast, making control difficult for operating personnel. The improved structures I, II, III, and IV here have overcompensate flow forces of 37.1N, 42.5N, 31.2N, and 21.4N respectively; these forces will add to the reset spring force, and along with the thrust of operating personnel, help accelerate the reset process. As the overcompensate flow forces are rather small, there is no cause for over-expedite of the spool valve reset process.

VI. CONCLUSION

From the study, we can conclude: firstly, the peak value of steady-state flow force always comes under the conditions of a large flow and a small opening of port P-T_1; secondly, when the peak value of flow force is greater than the value of reset spring force, spool clamping will occur; thirdly, the key to decreasing the peak value of flow force is to reduce impact on the spool valve wall; fourthly, the peak value of improved structure I's flow force is reduced by 17.8% in comparison with the original structure, of which effects of improvement were poor. Meanwhile, the peak value of improved structures II, III and IV's flow forces are reduced by 60.6%, 61.6% and 55.7% respectively in comparison with the original structure, which can effectively reduce the peak value of the spool valve, so as to avoid spool clamping. Last but not least, rational joint simulation process is the key to achieving accurate computational fluid dynamics (CFD) results, which should be strongly considered.

REFERENCES

[1] T. Jiang, M. Xia, and A. Wang, "A robust evaluation method of micro characteristics for directional control valve of hydraulic excavators," *J. Xi'an Jiaotong Univ.*, vol. 50, no. 2, pp. 118–123, Feb. 2016.

[2] R. Amirante, P. G. Moscatelli, and L. A. Catalano, "Evaluation of the flow forces on a direct (single stage) proportional valve by means of a computational fluid dynamic analysis," *Energy Convers. Manage.*, vol. 48, no. 3, pp. 942–953, 2007.

[3] G. Del Vescovo and A. Lippolis, "Three-dimensional analysis of flow forces on directional control valves," *Int. J. Fluid Power*, vol. 4, no. 2, pp. 15–24, 2003.

[4] N. Z. Aung, Q. Yang, M. Chen, and S. Li, "CFD analysis of flow forces and energy loss characteristics in a flapper-nozzle pilot valve with different null clearances," *Energy Convers. Manage.*, vol. 83, no. 7, pp. 284–295, 2014.

[5] M. O. Abdalla, T. Nagarajan, and M. H. Fakhruldin, "Numerical study of flow field and energy loss in hydraulic proportional control valve," in *Proc. Nat. Postgraduate Conf.*, Sep. 2011, pp. 1–6.

[6] M. Simic and N. Herakovic, "Reduction of the flow forces in a small hydraulic seat valve as alternative approach to improve the valve characteristics," *Energy Convers. Manage.*, vol. 89, pp. 708–718, Jan. 2015.

[7] R. Amirante, L. A. Catalano, C. Poloni, and P. Tamburrano, "Fluid-dynamic design optimization of hydraulic proportional directional valves," *Eng. Optim.*, vol. 46, no. 10, pp. 1295–1314, 2014.

[8] N. Z. Aung, P. Jinghui, and L. Songjing, "Reducing the steady flow force acting on the spool by using a simple jet-guiding groove," in *Proc. IEEE Int. Conf. Fluid Power Mechatronics*, Aug. 2015, pp. 289–294.

[9] G. Del Vesoco and A. Lippolis, "A review analysis of unsteady forces in hydraulic valves," *Int. J. Fluid Power*, vol. 7, no. 3, pp. 29–39, 2006.

[10] G. Zhang, J. Huang, and R. Qiu, "Evaluation of the flow force on an electro-hydraulic proportional valve based on CFD analysis," *J. Mach. Des.*, vol. 27, no. 6, pp. 93–96, 2010.

[11] S. Qing, J. Hong, W. Jinlin, and X. Hao, "Calculation for flow force of electro-hydraulic proportional valve in opening process," *Chin. Hydraul. Pneum.*, no. 11, pp. 30–34, 2015.

[12] N. Herakovič, "Flow-force analysis in a hydraulic sliding-spool valve," *Strojarstvo, časopis za teoriju i praksu u strojarstvu*, vol. 51, no. 6, pp. 555–564, 2009.

[13] M. Borghi, M. Milani, and R. Paoluzzi, "Stationary axial flow force analysis on compensated spool valves," *Int. J. Fluid Power*, vol. 1, no. 1, pp. 17–25, 2000.

[14] E. Lisowski, W. Czyzycki, and J. Rajda, "Three dimensional CFD analysis and experimental test of flow force acting on the spool of solenoid operated directional control valve," *Energy Convers. Manage.*, vol. 70, pp. 220–229, Jun. 2013.

[15] E. Lisowski, G. Filo, and J. Rajda, "Pressure compensation using flow forces in a multi-section proportional directional control valve," *Energy Convers. Manage*, vol. 103, pp. 1052–1064, Oct. 2015.

[16] W. Jia and C. Yin, "Notice of Retraction CFD simulation with fluent and experimental study on the characteristics of spool valve orifice," in *Proc. IEEE Int. Conf. Comput. Eng. Technol.*, Apr. 2010, pp. 590–594.

[17] S. Tac-Won and I. Barakat, "Computational analysis of the flow characteristics of drug-eluting stents," in *Proc. C. Korean Soc. Mech. Eng. Conf.*, Chugye, South Korea, Nov. 2011, pp. 1755–1759.

[18] H. Ji, X. Fu, and H.-Y. Yang, "Analysis and calculation on typical shape orifice areas in hydraulic valves," *J. Mach. Tool Hydraul.*, vol. 31, no. 5, pp. 14–16, 2003.

[19] W. Dongsheng, "Investigation into flow coefficient of orifice and calculation of steady ow force of spool valve with notches," M.S. thesis, Dept. Mech. Elect. Eng., Lanzhou Univ. Technol., Lanzhou, China, 2008.

[20] H. Ji, D.-S. Wang, D.-L. Ding, Z.-S. Tan, and X.-P. Liu, "Calculation method of orifice area of spool valve with notches," *J. Lanzhou Univ. Technol.*, vol. 34, no. 3, pp. 48–51, 2008.

[21] H. Y. Qing, S. Sonil, and K. Aniruddha, "Flow forces investigation through computational fluid dynamics and experimental study," in *Proc. 9th Int. Fluid Power Conf. (IFK)*, Aachen, Germany, 2014, pp. 101–109.

[22] E. Lisowski and J. Rajda, "CFD analysis of pressure loss during flow by hydraulic directional control valve constructed from logic valves," *Energy Convers. Manage.*, vol. 65, pp. 285–291, Jan. 2013.

[23] Q. Chen and B. Stoffel, "CFD simulation of a hydraulic servo valve with turbulent flow and cavitation," in *Proc. ASME/JSME Pressure Vessels Piping Conf.*, 2004, pp. 710–712.

[24] D. Wu, S. Li, and P. Wu, "CFD simulation of flow-pressure characteristics of a pressure control valve for automotive fuel supply system," *Energy Convers. Manage.*, vol. 101, pp. 658–665, Sep. 2015.

[25] J. Hong, C. Yong, W. Zhengrong, and W. Yang, "Numerical analysis of temperature rise by throttling and deformation in spool valve," in *Proc. IEEE Int. Conf. Fluid Power Mechatronics*, Aug. 2011, pp. 752–756.

[26] X. Pan, G. Wang, and Z. Lu, "Flow field simulation and a flow model of servo-valve spool valve orifice," *Energy Convers. Manage.*, vol. 52, no. 10, pp. 3249–3256, 2011.

[27] H. Chattopadhyay, A. Kundu, B. K. Saha, and T. Gangopadhyay, "Analysis of flow structure inside a spool type pressure regulating valve," *Energy Convers. Manage.*, vol. 53, no. 1, pp. 196–204, 2012.

[28] T.-J. Park and Y.-G. Hwang, "Effect of groove sectional shape on the lubrication characteristics of hydraulic spool valve," *Tribol. Online*, vol. 5, no. 5, pp. 239–244, 2010.

[29] Y. Ye, C.-B. Yin, X.-D. Li, W.-J. Zhou, and F.-F. Yuan, "Effects of groove shape of notch on the flow characteristics of spool valve," *Energy Convers. Manage.*, vol. 86, no. 5, pp. 1091–1101, 2014.

[30] G. Palau-Salvador, P. González-Altozano, I. Balbastre-Peralta, and J. Arviza-Valverde, "Improvement in a control valve geometry by CFD techniques," in *Proc. Pipeline Division Specialty Conf.*, 2005, pp. 202–215.

[31] M. Borghi, M. Milani, and R. Paoluzzi, "Influence of notch shape and number of notches on the metering characteristics of hydraulic spool valves," *Int. J. Fluid Power*, vol. 6, no. 2, pp. 5–18, 2005.

[32] D. Gao, "Investigation of flow structure inside spool valve with Fem and Piv methods," *Int. J. Fluid Power*, vol. 5, no. 1, pp. 51–66, 2004.

[33] H.-P. Zhang, "Correction for some wrong opinions about flow forces," *Hydraul. Pneum. Seals*, vol. 30, no. 9, pp. 10–15, 2010.

[34] J. Hong *et al.*, "Control method for steady-state flow force of open center multi-way valve," *J. Lanzhou Univ. Technol.*, vol. 44, no. 6, 2018.

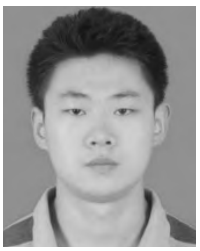

CHEN QIANPENG was born in Jiuquan, China, in 1989. He received the B.S. degree in mechanical design and automation from the Lanzhou University of Technology, Lanzhou, China, in 2013, and the M.S. degree in mechatronic engineering in 2017 from the Lanzhou University of Technology, Lanzhou, where he is currently pursuing the Ph.D. degree. His research interests include modern hydraulic elements and hydraulic transmission.

He has published one academic paper. He has applied for three patents for invention, of which one of the patents has been authorized.

JI HONG was born in Ningshan, Shanxi, China, in 1972. He received the B.S. and M.S. degrees in hydraulic transmission and control from the Lanzhou University of Technology, Lanzhou, in 1996 and the Ph.D. degree in hydraulic transmission and control from the National Key Laboratory, Zhejiang University of technology, Zhejiang, in 2005. He is currently a Professor, a Ph.D. Supervisor, and the Dean of the College of Energy and Power Engineering, Lanzhou University of Technology.

He has published over 80 papers in famous academic publications, of which there are approximately 30 papers indexed by SCI or EI. He holds eight authorized patents. He has undertaken three projects from the National Natural Science Foundation of China. His research direction is modern hydraulic elements and construction machinery hydraulic technology. He has focused on the basic theory and innovative technology of modern hydraulic elements for a long period of time.

ZHU YI was born in Wuhan, China, in 1992. She received the degree in processing units and control engineering from the Wuhan Institute of Technology, Wuhan, in 2014. She is currently pursuing the master's degree in power engineering with the Lanzhou University of Technology, Lanzhou. She was an Engineering Technician with Yichang Jiangxia Marine Machinery Co., Ltd., from 2014 to 2015. Her research interests are focused on hydraulic components analysis.

YANG XUBO was born in Xianyang, China, in 1991. He received the B.S. degree in mechanical design, manufacturing and automation from Yulin University, Yulin, in 2015. He is currently pursuing the master's degree in mechatronic engineering with the Lanzhou University of Technology, Lanzhou. He holds three patents for invention and eight patents for utility models which have been authorized. His research mainly focuses on hydraulic components analysis.